# CMS Physics Analysis Summary

Contact: cms-pag-conveners-b2g@cern.ch 2019/03/17

# Statistical combination of CMS searches for heavy resonances decaying to a pair of bosons or leptons at $\sqrt{s} = 13$ TeV

The CMS Collaboration

## Abstract

The statistical combination of searches for heavy resonances decaying to a pair of bosons or leptons is presented. The data sample corresponds to an integrated luminosity of 35.9 fb$^{-1}$ collected in 2016 by the CMS experiment at the CERN LHC from proton-proton collisions at a center-of-mass energy of 13 TeV. The data are found to be consistent with background expectations. The exclusion limits set in the context of a spin-1 heavy vector triplet framework and spin-2 Bulk Graviton models are the most stringent to date presented by CMS. In a scenario with mass-degenerate W′ and Z′ resonances, heavy vector bosons with mass below 4.5 TeV are excluded at a 95% confidence level if the dominant couplings are to the standard model gauge bosons, and 5.0 TeV if the resonances couple predominantly to fermions.

# 1 Introduction

Over the past half-century, searches for progressively heavier resonances in two-body decays have resulted in discoveries of several new states at particle colliders. At the LHC, searches for massive gauge bosons (W′ and Z′, collectively referred to as V′) that couple through electroweak (EW) interaction to SM particles have been performed by ATLAS and CMS in final states with two SM bosons [1–18], two leptons [19–22], two light-flavored quarks [23] or heavy flavor quarks [24–28], setting limits on the mass and the couplings of the resonances. The new states may couple predominantly to either SM fermions, as in the case of minimal W′ and Z′ models [29–31], or the SM bosons, as in strongly coupled composite Higgs and little Higgs models [32–38]. Warped extra dimensional (WED) models also provide a candidate for large-mass resonances such as the spin-2 first Kaluza-Klein (KK) excitation of the graviton (G) [39–41], which has a sizable branching fraction to pairs of W, Z, and H bosons.

This article describes the statistical combination of CMS searches for heavy resonances decaying to a pair of bosons or leptons [1–10], and provides the most competitive exclusion limits from the CMS experiment on beyond-the-SM theories that foresee heavy vector resonances or a Bulk Graviton. Due to the resonances having large masses that exceed 1 TeV, the SM bosons produced in their decay should have large Lorentz boosts. The decay products of the SM bosons are thus very collimated, requiring dedicated reconstruction techniques for their identification and reconstruction. In the case of hadronic decays, the pair of quarks are reconstructed using a single large-cone jet with a two-pronged structure originating from the two hadronized quarks. Additionally, Higgs boson decays may also be identified by tagging the b quarks originating from its decay. In models where the heavy vector bosons couple predominantly to fermions, the contribution from leptonic decays $W' \to \ell\nu$ and $Z' \to \ell\ell$ dominates, and these channels are included in the combination [19, 20]. The analyses considered are based on 35.9 $\text{fb}^{-1}$ of integrated luminosity at $\sqrt{s} = 13$ TeV collected during the 2016 data-taking period by the CMS experiment. A similar combination performed on a comparable dataset has been recently published by ATLAS [42].

# 2 The CMS detector and event reconstruction

The CMS detector features a silicon pixel and strip tracker, a lead tungstate crystal electromagnetic calorimeter (ECAL), and a brass and scintillator hadron calorimeter (HCAL), each composed of a barrel and two endcap sections. Forward calorimeters extend the pseudo-rapidity coverage up to $|\eta| < 5.2$. These detectors reside within the superconducting solenoid, which provides a magnetic field of 3.8 T. Muons are measured in gas-ionization detectors embedded in the steel flux-return yoke outside the solenoid. A detailed description of the CMS detector, together with a definition of the coordinate system and the relevant kinematic variables, can be found in Ref. [43].

The information from the various elements of the CMS detector is used by the particle-flow (PF) algorithm [44] to identify stable particles reconstructed in the detector as electrons, muons, photons, and charged or neutral hadrons. The energy of electrons is determined from a combination of the electron momentum, as determined by the tracker, the energy of the corresponding ECAL cluster, and the energy sum of all bremsstrahlung photons spatially compatible with originating from the electron track [45]. The energy of muons is obtained from the curvature of the corresponding track [46]. Hadronically decaying $\tau$ leptons are reconstructed by combining one or three charged particle PF candidates with up to two neutral pion candidates [47]. The energy of charged hadrons is determined from a combination of their momentum measured in

the tracker and the matching ECAL and HCAL energy deposits, corrected for zero-suppression effects and for the response function of the calorimeters to hadronic showers. Finally, the energy of neutral hadrons is obtained from the corresponding corrected ECAL and HCAL energy.

Jets are reconstructed from PF candidates clustered with the anti-$k_T$ algorithm [48] and a distance parameter $R = 0.4$ (AK4 jets) or $R = 0.8$ (AK8 jets) using the FASTJET 3.0 package [49]. The four-momenta of the AK4 and AK8 jets are obtained by clustering candidates passing the charged hadron subtraction (CHS) algorithm [50]. The contribution of neutral particles originating from pileup interactions is proportional to the jet area and is estimated using the median area method implemented in FASTJET [51], and then subtracted from the jet energy. The jet energy resolution, after the application of corrections to the jet energy, amounts to 4% at 1 TeV [52]. The associated missing transverse momentum $\vec{p}_T^{\,\text{miss}}$ is taken as the negative vector sum of the $p_T$ of the AK4 jets.

The investigation of the AK8 jet mass ($m_j$) and substructure relies on the pileup per particle identification (PUPPI) algorithm [50, 53]. The contributions from soft radiation and additional interactions are removed using the soft-drop algorithm [54, 55], with algorithm parameters $\beta = 0$ and $z_{cut} = 0.1$. Dedicated mass corrections, derived from simulation and data in a region enriched with $t\bar{t}$ events with merged $W(q\overline{q'})$ decays, are applied to the jet mass in order to remove residual jet $p_T$ dependence [5, 56], and to match the jet mass scale and resolution observed in data. The measured soft-drop jet mass resolution is approximately 10%. Exclusive $m_j$ intervals $m_W, m_Z, m_H$, which range from 65 to 85, 85 to 105, and 105 to 135 GeV, respectively, are defined according to the nominal mass of the SM bosons.

The N-subjettiness [57] variable $\tau_{21}$ is used to identify jets that result from the merger of more than one parton jet. The performance of selection criteria using $\tau_{21}$ is measured from data in a sample enriched in $t\bar{t}$ events [56]. The decay of a Higgs boson to a pair of b quarks are identified using two different b tagging algorithms, depending on the background composition. The first consists of a dedicated b tagging discriminator, specifically designed to identify a pair of b quarks clustered in a single jet [58]. The second relies on the splitting of the AK8 jet into two subjets, and the application of the combined secondary vertex algorithm [59] to the subjets.

## 3 Signal models and simulation

The response of the CMS detector to the production and decay of the heavy resonances is evaluated through simulated events, which are reconstructed with the same algorithms used in collision data. The spin-1 gauge bosons, $W'$ and $Z'$, are simulated at leading order (LO) using the MADGRAPH5_aMC@NLO v2.4.2 matrix element generator [60] within the heavy vector triplet (HVT) framework [61], which introduces a triplet of heavy vector bosons, one neutral ($Z'$) and two electrically charged ($W'^{\pm}$), which are degenerate in mass. In the HVT framework, $g_V$ is the coupling strength of the new interaction, $c_H$ is the coupling between the HVT bosons, the Higgs boson, and longitudinally polarized SM vector bosons, $c_F$ is the coupling between the HVT bosons and the SM fermions, and $g$ is the SM $SU(2)_L$ gauge coupling. The coupling strength of the heavy vector bosons to SM bosons and fermions is determined by combinations $g_V c_H$ and $g^2 c_F / g_V$, respectively. The HVT framework is presented in two scenarios, henceforth referred to as model A and model B, depending on the couplings to the SM particles [61]. In the former, the coupling strengths to the SM bosons and fermions are comparable and the new particles decay primarily to fermions. In the latter, the couplings to the SM fermions are small, and the branching fraction to the SM bosons is nearly 100%. Samples are simulated in HVT model B, and different mass hypotheses in the range of 800 to 4500 GeV are considered, assuming a negligible resonance width compared to the experimental resolution.

The bulk graviton samples are simulated at LO with the same generator. In the bulk scenario [62, 63], the cross section and width of the graviton mainly depend on its mass and the ratio $\tilde{\kappa} \equiv \kappa/\overline{M}_{Pl}$, where $\kappa$ is a curvature factor of the model and $\overline{M}_{Pl}$ is the reduced Planck mass. The graviton signals are generated assuming $\tilde{\kappa} = 0.5$, which guarantees that the graviton resonance width is smaller than the experimental resolution.

The signal samples are generated using the NNPDF 3.0 [64] parton distribution functions (PDFs), and are interfaced with PYTHIA 8.205 [65, 66] for the parton showering and hadronization adopting the MLM matching scheme [67]. Additional pp interactions within the same or neighboring bunch crossings (pileup) are superimposed on the simulated processes, and the frequency distribution of the additional events is weighted to match the number of interactions per bunch crossing that was observed in 2016 data. Generated events are processed through a CMS detector simulation based on GEANT4 [68].

# 4 Search channels

Diboson and dilepton resonances have been sought in several final states, depending on the decay modes of the bosons. Searches have been performed targeting VV [4], VH [5], and HH final states [2, 10] with both bosons decaying to quarks. The two bosons are reconstructed as two-pronged large-cone jets, recoiling against each other. The diboson resonance is reconstructed from the dijet invariant mass. The W and Z bosons are identified through their mass and $\tau_{21}$, and b tagging is used to identify H boson candidates. Although the signal yield is large, due to the large branching fraction of the bosons decaying to hadrons or b quarks, these channels are subject to the overwhelming background represented by QCD multijet production. In the VV and VH analyses, the background is estimated directly from data, assuming that the background invariant mass distribution can be described by a smooth, parametrizable, monotonically decreasing function. The signal template, based on a Gaussian core, is fitted to the data simultaneously with the background function. The HH analyses also use an additional region in the fit, derived by inverting the b tagging selection on the H candidates to constrain the parameters of the background function.

Searches for VV, VH, and HH resonances have been performed in final states where one of the SM bosons decays to leptons ($\mathrm{Z} \to \nu\nu, \mathrm{W} \to \ell\nu, \mathrm{Z} \to \ell\ell$, or $\mathrm{H} \to \tau\tau$), and the other to quarks ($\mathrm{W}, \mathrm{Z} \to \mathrm{q\bar{q}}$ or $\mathrm{H} \to \mathrm{b\bar{b}}$) [3, 6–9]. These final states represent an attractive alternative to hadronic channels, thanks to the large selection efficiency and the natural discrimination of the multijet background due to the presence in the signal of high-momenta, isolated leptons. The decay of a Z boson to neutrinos can be identified by a large amount of $p_{\mathrm{T}}^{\mathrm{miss}}$, and the resonance mass can be inferred from the transverse mass summed with the visible jet. For the $\mathrm{W} \to \ell\nu$ decay, a single, isolated lepton and a moderate amount of missing energy will emerge, and the vector boson can be reconstructed by imposing a constraint on the W boson mass to recover the longitudinal momentum of the neutrino. In $\mathrm{Z} \to \ell\ell$ decays, two opposite sign, same-flavor leptons whose invariant mass is compatible with the Z boson mass $m_Z$ are used to accurately determine the Z boson four-momentum. Higgs bosons decaying to $\tau$ leptons are identified through dedicated hadronic $\tau$ reconstruction and their expected value of isolation from other particles [8]. The hadronically decaying bosons are reconstructed as AK8 jets. In the semi-leptonic analyses, the main V+jets background is estimated from a fit to data in the jet mass sidebands of the hadronic jet, and extrapolated to the signal region using a transfer function ("$\alpha$-function") derived from simulated samples. Since the background contribution from top quark pair production can be large, its normalization is derived from appropriate control regions. In addition, the $\mathrm{WV} \to \ell\nu\mathrm{q\bar{q}}$ [3] analysis introduces a novel signal extraction

method based on a two-dimensional fit to data. The backgrounds are separated into non-resonant or resonant categories depending on the presence of genuine resonances (W bosons and top quarks) in the jet mass spectrum, and fitted simultaneously in the space of the jet mass and the resonance mass, accounting for the correlation between the two variables.

Searches for diboson resonances decaying to a pair of Z bosons have been performed in fully leptonic final states, with one boson decaying $Z \to \ell\ell$ and the other $Z \to \nu\nu$ [1]. The presence of the bosons defines a very clean final state with reduced backgrounds, but the small branching fraction makes this channel competitive only for low mass values.

The decay of a heavy resonance to a pair of fermions may be sizable if the couplings to SM fermions are large. If the resonance is electrically charged, as is the $W'^{\pm}$, the decay to an electron or muon, and a neutrino yields a broad excess in the transverse mass spectrum [20]. If the new state is neutral, a narrow resonance would emerge from the dielectron or dimuon invariant mass [19]. The analyses of these fermionic decays extend to masses above 5 TeV, and employ dedicated selection techniques to identify and measure leptons with very high momenta.

## 5 Event selection

The analyses entering in the combination are required to be statistically independent. The considered channels are orthogonal due to exclusive selections on lepton number and flavor, number of AK8 jets, and jet mass intervals. Analyses with hadronic final states reject events with isolated leptons or large missing transverse energy reconstructed in the detector. Channels that share the same lepton multiplicity avoid overlaps by selecting different jet mass intervals. The $W' \to \ell\nu$ search does not share any event with the $W' \to VW$ and $W' \to WH$ selections due to requirements on the angular separation between the missing energy and the lepton, $\Delta\phi(\ell, \vec{p}_T^{\,\text{miss}})$. The $Z' \to \ell\ell$ analysis selects events with dilepton invariant mass larger than 120 GeV, which is incompatible with the $70 < m_{\ell\ell} < 110$ GeV selection used in the diboson channels, in which the Z boson is on-shell. Finally, the two searches for resonant HH bosons decaying to b quarks manually remove common events. In the $WV \to \ell\nu q\bar{q}$ channel [3] the background is estimated using the 2D fit technique, which scans the full jet mass range, and therefore is not independent from the $WH \to \ell\nu b\bar{b}$ channel. For this reason, in the $W'$, $Z'$, and $V'$ interpretations, where the two signals simultaneously coexist, the alternate "$\alpha$-function" background estimation is used instead [3]; this method only considers events in the jet mass regions of the W and Z bosons, preventing the double-counting of data events in the H-mass region. The results of the alternate background estimation method is consistent with the ones derived with the 2D fit, but about 10% less stringent. The main selections that define the orthogonality among the analyses are summarized in Table 1.

## 6 Systematic uncertainties

The systematic uncertainties that affect the normalization or shape of the background distributions are considered as uncorrelated, since the background estimation is performed in statistically independent regions. The uncertainties arising from reconstruction and calibration are modeled with a single nuisance parameter per uncertainty, in common across different measurements, when applicable, and are thus correlated among the different channels. These include the uncertainties on the jet energy and resolution, the electron, muon and $\tau$ lepton reconstruction, identification, and measurement of the energy or the momentum. The uncertainties on the identification of the hadronically decaying SM bosons are the dominant ones in the final states with at least one such decay, and originate from the jet mass and resolution, the selection

Table 1: Summary of the main selections that guarantee the orthogonality between analyses. The symbol $\ell$ represents an electron or a muon; $\tau$ leptons are considered separately. The AK4 b jets are additional b tagged AK4 jets that do not geometrically overlap with AK8 jets.

| Final state | $\ell$ | $\tau$ | AK8 jets | AK8 jet mass SR | AK4 b jets | other selections |
|---|---|---|---|---|---|---|
| $VV \to q\bar{q}q\bar{q}$ [4] | veto | - | 2 | $2 \times [m_W, m_Z]$ | - | |
| $VZ \to \nu\nu q\bar{q}$ [7] | veto | veto | 1 | $1 \times m_V$ | veto | |
| $VW \to \ell\nu q\bar{q}$ [3] | 1 | - | 1 | $m_j$ shape/$1 \times [m_W, m_Z]$ | veto | $\Delta\phi(W, j) > 2$ |
| $VZ \to \ell\ell q\bar{q}$ [9] | 2 | - | 1 | $1 \times m_V$ | - | $70 < m_{\ell\ell} < 110\,\text{GeV}$ |
| $ZZ \to \ell\ell\nu\nu$ [1] | 2 | - | - | - | - | |
| $VH \to q\bar{q}b\bar{b}$ [5] | veto | veto | 2 | $1 \times [m_W, m_Z]$, $1 \times m_H$ | - | |
| $VH \to \nu\nu b\bar{b}$ [6] | 0 | veto | 1 | $1 \times m_H$ | veto | |
| $VH \to \ell\nu b\bar{b}$ [6] | 1 | veto | 1 | $1 \times m_H$ | veto | $\Delta\phi(\ell, p_T^{miss}) < 2$ |
| $VH \to \ell\ell b\bar{b}$ [6] | 2 | veto | 1 | $1 \times m_H$ | - | $70 < m_{\ell\ell} < 110\,\text{GeV}$ |
| $VH \to \tau\tau b\bar{b}$ [8] | - | 2 | 1 | $1 \times [m_W, m_Z]$ | veto | |
| $HH \to b\bar{b}b\bar{b}$ [2] | - | - | 2 | $2 \times m_H$ | - | shared events are |
| $HH \to b\bar{b}b\bar{b}$ [10] | - | - | 1 | $1 \times m_H$ | 2 | manually removed |
| $HH \to \tau\tau b\bar{b}$ [8] | - | 2 | 1 | $1 \times m_H$ | veto | |
| $\ell\nu$ [20] | 1 | - | - | - | - | $\Delta\phi(\ell, E_T^{miss}) > 2.5$ |
| $\ell\ell$ [19] | 2 | - | - | - | - | $m_{\ell\ell} > 120\,\text{GeV}$ |

on the N-subjettiness, the b tagging, or a combination of the two. Uncertainties covering the extrapolation to very high jet $p_T$ of the N-subjettiness selection and the selection of events in jet mass window of the Higgs boson are also included. The uncertainties on the proton-proton inelastic cross section, the delivered luminosity during the 2016 data-taking, and the kinematic acceptance of the final-state particles affect the signal normalization, and are taken as correlated among channels as well. Theory uncertainties on the cross section and signal geometric acceptance are considered related to the choice of PDFs used by the event generators [69] and are derived according to the PDF4LHC recommendations [69], as well as uncertainties on the factorization and renormalization scales, obtained by varying the corresponding scales up and down by a factor of 2. The impact on the signal cross section can be as large as 50%, depending on the signal mass and the initial state ($q\bar{q}$ or $gg$). These uncertainties are not profiled in the fit when presenting the results as upper limits on the cross sections, and are included in the uncertainty band of the theoretical cross section line. When placing constraints on the HVT model parameters, the uncertainties are instead profiled in the fit.

# 7 Results and interpretation

No significant excess above the background expectation has been observed in the individual channels, and upper limits at 95% confidence level (CL) are set on the cross sections of heavy resonances using the modified frequentist approach ($CL_s$), and taking the likelihood as the test statistic [70–72] in the asymptotic approximation [73]. This approximation leads to up to 30% stronger limits compared to the $CL_s$, depending on the resonance mass. Systematic uncertainties are treated as nuisance parameters that are modeled through log-normal priors.

The exclusion limits on the cross section of each diboson final state (WW, WZ, ZZ, WH, ZH, HH) are depicted in Fig. 1 according to the spin of the exotic particle. The generated signal may be either a spin-1 heavy vector (W′ or Z′, as in the HVT model) or a spin-2 boson (as in Graviton models). In fact, the spin and polarization of the heavy resonance affect the final state, signal acceptance, and selection efficiencies. The exclusion limits are presented up to 4.5 TeV, because above these value the background estimation procedure used in diboson analyses becomes less reliable due to the lack of events in data.

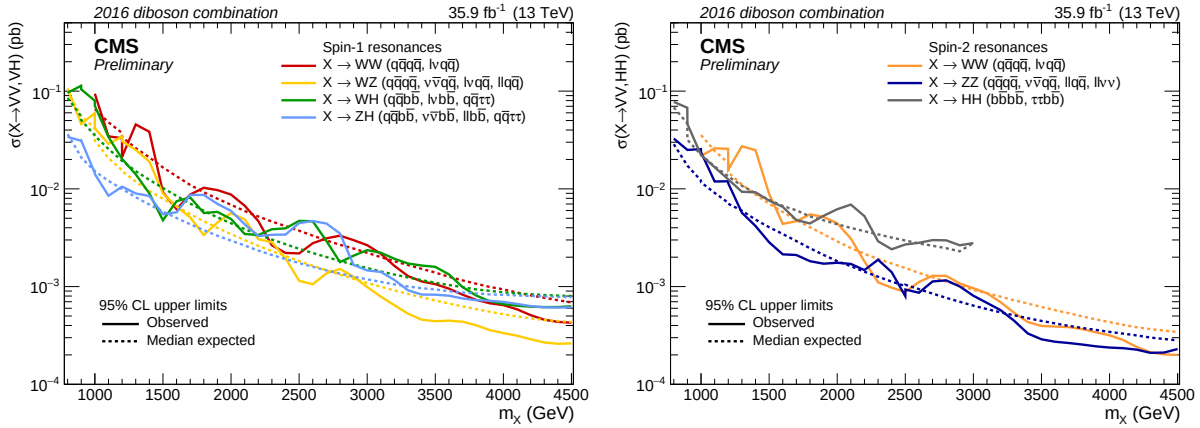


Figure 1: Observed and expected 95% CL upper limits on the product of the cross section and branching ratio of a spin-1 (left) or spin-2 resonance (right) decaying to a pair of bosons.

The combined exclusion limits for the spin-1 singlet hypotheses (W′ or Z′) in the HVT model B framework, where the branching fractions to SM bosons are dominating, are shown in Fig. 2. In this scenario, the contribution of the dilepton channels is negligible due to their branching fraction of the order of few permil. The contribution from VH decays to VV channels, caused by an underestimation of $m_{\mathrm{j}}$, is also considered. The predictions of the HVT model B are superimposed on the exclusion limits, and a W′ with mass lower than 4.3 TeV, and a Z′ with mass lower than 3.7 TeV are excluded at 95% CL.

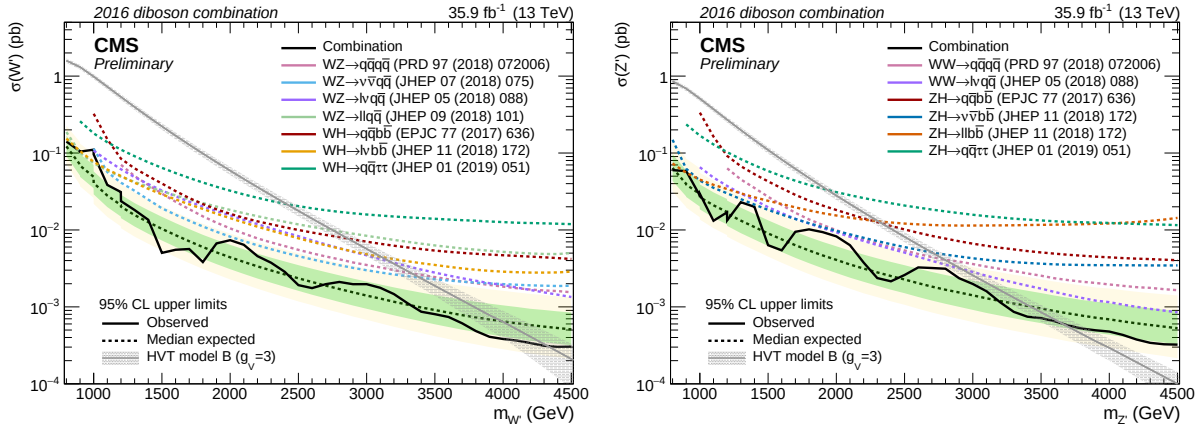


Figure 2: Observed and expected 95% CL upper limits on the W′ (left) and Z′ cross section (right) as a function of the W′ and Z′ resonance mass. The inner green and outer yellow bands represent the $\pm 1$ and $\pm 2$ standard deviation variations on the expected limits of the statistical combination of the considered VV and VH channels. The expected limit of the single channels is represented by the colored dashed lines. The solid curves and their shaded areas correspond to the cross section predicted by the HVT models B and the relative uncertainties.

The HVT hypothesis is tested by combining all diboson channels in Fig. 3, and a mass-degenerate state with mass below 4.5 TeV can be excluded with the considered dataset in HVT model B. The dilepton resonances provide the most stringent results within the HVT model A framework, and are combined with the diboson searches in Fig. 3. A heavy triplet of V′ resonances is excluded up to a mass of 5.0 TeV. The most significant excesses in the W′, Z′, V′, and G combinations have a local (global) significance of 2.8 (1.3), 2.6 (0.7), 2.4 (0.5), and 2.2 (0.7) standard deviations, respectively. The significances are derived in the asymptotic approximation [73].

The exclusion limits on the resonance cross section shown in Fig. 3 are also interpreted as a limit

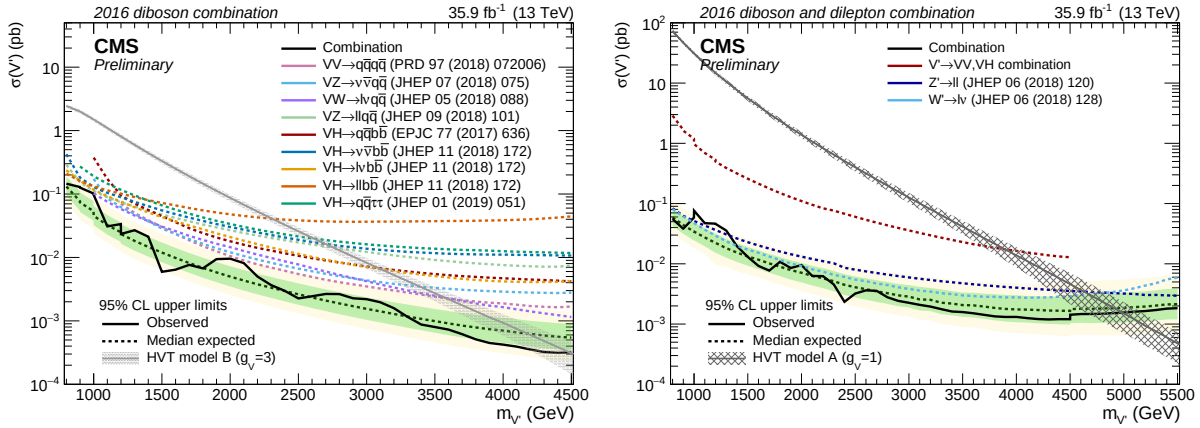


Figure 3: Observed and expected 95% CL upper limit on the cross section as a function of the HVT triplet mass, for the combination of all the considered channels, in the HVT model B (left) and model A (right). The inner green and outer yellow bands represent the $\pm 1$ and $\pm 2$ standard deviation variations on the expected limit. The solid curves and their shaded areas correspond to the cross sections predicted by the HVT models A and B and the relative uncertainties.

in the $\left[g_{\mathrm{V}}c_{\mathrm{H}},\ g^2c_{\mathrm{F}}/g_{\mathrm{V}}\right]$ plane of the HVT parameters. The excluded region of the parameter space for narrow resonances obtained from the combination of all the considered channels is shown in Fig. 4. The dilepton and diboson searches are able to constrain different regions of the parameter space. Including the dilepton searches allows for the exclusion of the region where the coupling to the SM bosons approaches zero. In this interpretation, the ratio between the W′ and Z′ cross sections is assumed to be determined by the ratio of the partonic luminosities, and to loosely depend on the model parameters. The fraction of the parameter space where the natural width of the resonances is larger than the average experimental resolution of 5%, and the narrow width approximation is not valid, is also indicated in Fig. 4. The extent of the parameter space excluded significantly improves on the reach of the previous $\sqrt{s} = 8$ and 13 TeV CMS combination [74], which excluded a triplet of heavy resonances up to 2.4 TeV in model B. These results represent the most stringent limits on these models presented by CMS, and are comparable with the ATLAS combination of similar final states [42].

In the spin-2 bulk graviton model, the WW, ZZ, and HH channels are combined, setting upper limits of up to 1.1 fb on the cross section of a graviton with mass of 4.5 TeV. In the $\tilde{\kappa} = 0.5$ scenario, a graviton with mass smaller than 850 GeV is excluded at 95% CL, as shown in Fig. 5. Larger $\tilde{\kappa}$ values increase the production cross sections, but also the resonance width, which may be comparable or larger than the experimental resolution. In these cases, the narrow width approximation is no longer valid.

# 8 Summary

The statistical combination of searches for heavy resonances decaying into a pair of vector bosons, a vector boson and a Higgs boson, two Higgs bosons, or a pair of leptons, has been presented. The searches are performed on the data collected by the CMS experiment at $\sqrt{s} =$ 13 TeV during 2016, and correspond to an integrated luminosity of 35.9 $\mathrm{fb}^{-1}$. In models with warped extra dimensions, upper limits of up to 1.1 fb at 95% CL are set on the production cross section of the spin-2 bulk graviton. For models with a triplet of narrow spin-1 resonances, heavy vector bosons with masses lower than 5.0 and 4.5 TeV are excluded at 95% CL in benchmark scenarios A and B, respectively.

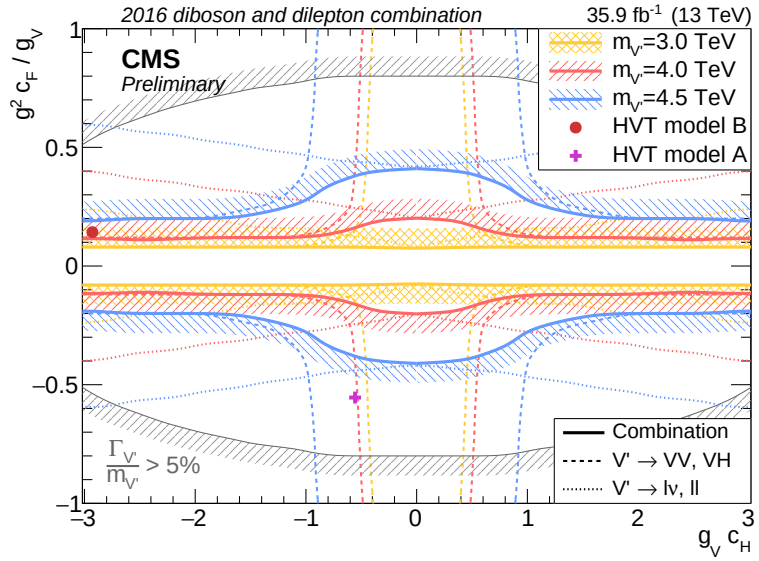


Figure 4: Observed exclusion limits in the HVT parameter plane $\left[g_V c_H,\ g^2 c_F/g_V\right]$ for three different resonance masses (3.0, 4.0, and 4.5 TeV) of the statistical combination (solid lines) of the dilepton (dotted lines) and diboson channels (dashed lines). The areas bounded by the thin gray contour lines correspond to the regions where the resonance natural width ($\Gamma_{V'}$) is predicted to be larger than the average experimental resolution (5%).

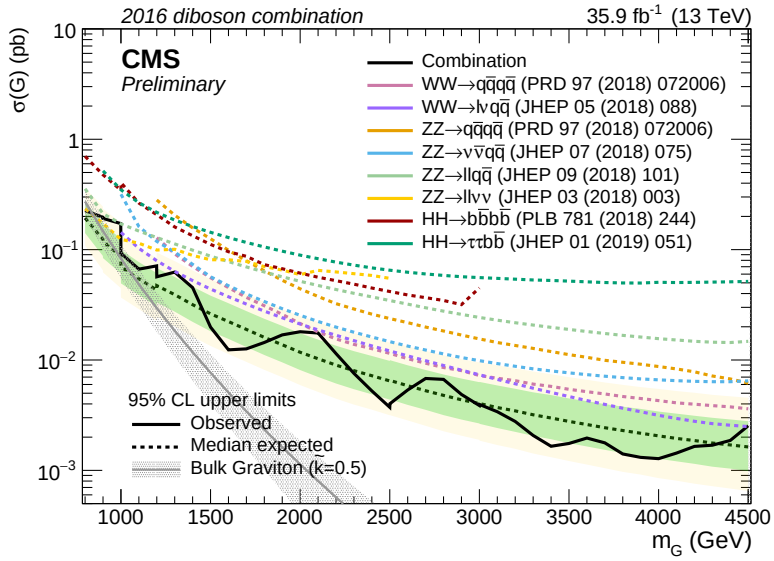


Figure 5: Observed and expected 95% CL upper limit on the cross section of the spin-2 Bulk Graviton as a function of its mass for the statistical combination of the WW, ZZ, and HH channels. The inner green and outer yellow bands represent the $\pm 1$ and $\pm 2$ standard deviation variations on the expected limit. The solid curve and its shaded area represent the cross section derived with the parameter $\tilde{\kappa} = 0.5$ and the associated uncertainty.

# References


[1] CMS Collaboration, "Search for ZZ resonances in the $2\ell 2\nu$ final state in proton-proton collisions at 13 TeV", *JHEP* **03** (2018) 003, doi:10.1007/JHEP03(2018)003, arXiv:1711.04370.

[2] CMS Collaboration, "Search for a massive resonance decaying to a pair of Higgs bosons in the four b quark final state in proton-proton collisions at $\sqrt{s} = 13$ TeV", *Phys. Lett. B* **781** (2018) 244–269, doi:10.1016/j.physletb.2018.03.084, arXiv:1710.04960.

[3] CMS Collaboration, "Search for a heavy resonance decaying to a pair of vector bosons in the lepton plus merged jet final state at $\sqrt{s} = 13$ TeV", *JHEP* **05** (2018) 088, doi:10.1007/JHEP05(2018)088, arXiv:1802.09407.

[4] CMS Collaboration, "Search for massive resonances decaying into $WW$, $WZ$, $ZZ$, $qW$, and $qZ$ with dijet final states at $\sqrt{s} = 13$ TeV", *Phys. Rev. D* **97** (2018), no. 7, 072006, doi:10.1103/PhysRevD.97.072006, arXiv:1708.05379.

[5] CMS Collaboration, "Search for heavy resonances that decay into a vector boson and a Higgs boson in hadronic final states at $\sqrt{s} = 13$ TeV", *Eur. Phys. J. C* **77** (2017) 636, doi:10.1140/epjc/s10052-017-5192-z, arXiv:1707.01303.

[6] CMS Collaboration, "Search for heavy resonances decaying into a vector boson and a Higgs boson in final states with charged leptons, neutrinos and b quarks at $\sqrt{s} = 13$ TeV", *JHEP* **11** (2018) 172, doi:10.1007/JHEP11(2018)172, arXiv:1807.02826.

[7] CMS Collaboration, "Search for a heavy resonance decaying into a Z boson and a vector boson in the $\nu\bar{\nu}\mathrm{q}\bar{\mathrm{q}}$ final state", *JHEP* **07** (2018) 075, doi:10.1007/JHEP07(2018)075, arXiv:1803.03838.

[8] CMS Collaboration, "Search for heavy resonances decaying into two Higgs bosons or into a Higgs boson and a W or Z boson in proton-proton collisions at 13 TeV", *JHEP* **01** (2019) 051, doi:10.1007/JHEP01(2019)051, arXiv:1808.01365.

[9] CMS Collaboration, "Search for a new heavy resonance decaying into a Z boson and a Z or W boson in $2\ell$2q final states at $\sqrt{s} = 13$ TeV", arXiv:1803.10093.

[10] CMS Collaboration, "Search for production of Higgs boson pairs in the four b quark final state using large-area jets in proton-proton collisions at $\sqrt{s} = 13$ TeV", arXiv:1808.01473.

[11] ATLAS Collaboration, "Search for $WW/WZ$ resonance production in $\ell\nu qq$ final states in $pp$ collisions at $\sqrt{s} = 13$ TeV with the ATLAS detector", *JHEP* **03** (2018) 042, doi:10.1007/JHEP03(2018)042, arXiv:1710.07235.

[12] ATLAS Collaboration, "Search for resonant $WZ$ production in the fully leptonic final state in proton-proton collisions at $\sqrt{s} = 13$ TeV with the ATLAS detector", arXiv:1806.01532.

[13] ATLAS Collaboration, "Search for heavy resonances decaying into $WW$ in the $e\nu\mu\nu$ final state in $pp$ collisions at $\sqrt{s} = 13$ TeV with the ATLAS detector", *Eur. Phys. J. C* **78** (2018), no. 1, 24, doi:10.1140/epjc/s10052-017-5491-4, arXiv:1710.01123.

[14] ATLAS Collaboration, "Searches for heavy $ZZ$ and $ZW$ resonances in the $\ell\ell qq$ and $\nu\nu qq$ final states in $pp$ collisions at $\sqrt{s} = 13$ TeV with the ATLAS detector", *JHEP* **03** (2018) 009, doi:10.1007/JHEP03(2018)009, arXiv:1708.09638.

[15] ATLAS Collaboration, "Search for heavy ZZ resonances in the $\ell^+\ell^-\ell^+\ell^-$ and $\ell^+\ell^-\nu\bar{\nu}$ final states using proton-proton collisions at $\sqrt{s} = 13$ TeV with the ATLAS detector", *Eur. Phys. J. C* **78** (2018), no. 4, 293, doi:10.1140/epjc/s10052-018-5686-3, arXiv:1712.06386.

[16] ATLAS Collaboration, "Search for heavy resonances decaying to a $W$ or $Z$ boson and a Higgs boson in the $q\bar{q}^{(\prime)}b\bar{b}$ final state in $pp$ collisions at $\sqrt{s} = 13$ TeV with the ATLAS detector", *Phys. Lett. B* **774** (2017) 494–515, doi:10.1016/j.physletb.2017.09.066, arXiv:1707.06958.

[17] ATLAS Collaboration, "Search for heavy resonances decaying into a $W$ or $Z$ boson and a Higgs boson in final states with leptons and $b$-jets in 36 fb$^{-1}$ of $\sqrt{s} = 13$ TeV $pp$ collisions with the ATLAS detector", *JHEP* **03** (2018) 174, doi:10.1007/JHEP03(2018)174, arXiv:1712.06518.

[18] ATLAS Collaboration, "Search for diboson resonances with boson-tagged jets in $pp$ collisions at $\sqrt{s} = 13$ TeV with the ATLAS detector", *Phys. Lett. B* **777** (2018) 91–113, doi:10.1016/j.physletb.2017.12.011, arXiv:1708.04445.

[19] CMS Collaboration, "Search for high-mass resonances in dilepton final states in proton-proton collisions at $\sqrt{s} = 13$ TeV", *JHEP* **06** (2018) 120, doi:10.1007/JHEP06(2018)120, arXiv:1803.06292.

[20] CMS Collaboration, "Search for high-mass resonances in final states with a lepton and missing transverse momentum at $\sqrt{s} = 13$ TeV", *JHEP* **06** (2018) 128, doi:10.1007/JHEP06(2018)128, arXiv:1803.11133.

[21] ATLAS Collaboration, "Search for a new heavy gauge boson resonance decaying into a lepton and missing transverse momentum in 36 fb$^{-1}$ of $pp$ collisions at $\sqrt{s} = 13$ TeV with the ATLAS experiment", *Eur. Phys. J. C* **78** (2018), no. 5, 401, doi:10.1140/epjc/s10052-018-5877-y, arXiv:1706.04786.

[22] ATLAS Collaboration, "Search for new high-mass phenomena in the dilepton final state using 36 fb$^{-1}$ of proton-proton collision data at $\sqrt{s} = 13$ TeV with the ATLAS detector", *JHEP* **10** (2017) 182, doi:10.1007/JHEP10(2017)182, arXiv:1707.02424.

[23] CMS Collaboration, "Search for narrow and broad dijet resonances in proton-proton collisions at $\sqrt{s} = 13$ TeV and constraints on dark matter mediators and other new particles", *JHEP* **08** (2018) 130, doi:10.1007/JHEP08(2018)130, arXiv:1806.00843.

[24] CMS Collaboration, "Search for resonant $\mathrm{t\bar{t}}$ production in proton-proton collisions at $\sqrt{s} = 13$ TeV", *Submitted to: JHEP* (2018) arXiv:1810.05905.

[25] CMS Collaboration, "Search for heavy resonances decaying to a top quark and a bottom quark in the lepton+jets final state in proton-proton collisions at 13 TeV", *Phys. Lett. B* **777** (2018) doi:10.1016/j.physletb.2017.12.006, arXiv:1708.08539.

[26] ATLAS Collaboration, "Search for resonances in the mass distribution of jet pairs with one or two jets identified as $b$-jets in proton-proton collisions at $\sqrt{s} = 13$ TeV with the ATLAS detector", *Phys. Rev. D* **98** (2018) 032016, doi:10.1103/PhysRevD.98.032016, arXiv:1805.09299.

[27] ATLAS Collaboration, "Search for heavy particles decaying into top-quark pairs using lepton-plus-jets events in proton-proton collisions at $\sqrt{s} = 13$ TeV with the ATLAS detector", *Eur. Phys. J. C* **78** (2018), no. 7, 565, doi:10.1140/epjc/s10052-018-5995-6, arXiv:1804.10823.

[28] ATLAS Collaboration, "Search for $W' \to tb$ decays in the hadronic final state using pp collisions at $\sqrt{s} = 13$ TeV with the ATLAS detector", *Phys. Lett.B* **781** (2018) 327–348, doi:10.1016/j.physletb.2018.03.036, arXiv:1801.07893.

[29] C. Grojean, E. Salvioni, and R. Torre, "A weakly constrained W′ at the early LHC", *JHEP* **07** (2011) 002, doi:10.1007/JHEP07(2011)002, arXiv:1103.2761.

[30] V. D. Barger, W.-Y. Keung, and E. Ma, "A gauge model with light $W$ and $Z$ bosons", *Phys. Rev. D* **22** (1980) 727, doi:10.1103/PhysRevD.22.727.

[31] E. Salvioni, G. Villadoro, and F. Zwirner, "Minimal Z' models: present bounds and early LHC reach", *JHEP* **09** (2009) 068, doi:10.1088/1126-6708/2009/11/068, arXiv:0909.1320.

[32] R. Contino, D. Pappadopulo, D. Marzocca, and R. Rattazzi, "On the effect of resonances in composite Higgs phenomenology", *JHEP* **10** (2011) 081, doi:10.1007/JHEP10(2011)081, arXiv:1109.1570.

[33] D. Marzocca, M. Serone, and J. Shu, "General composite Higgs models", *JHEP* **08** (2012) 13, doi:10.1007/JHEP08(2012)013, arXiv:1205.0770.

[34] B. Bellazzini, C. Csaki, and J. Serra, "Composite Higgses", *Eur. Phys. J. C* **74** (2014) 2766, doi:10.1140/epjc/s10052-014-2766-x, arXiv:1401.2457.

[35] K. Lane and L. Pritchett, "The light composite Higgs boson in strong extended technicolor", *JHEP* **06** (2017) 140, doi:10.1007/JHEP06(2017)140, arXiv:1604.07085.

[36] T. Han, H. E. Logan, B. McElrath, and L.-T. Wang, "Phenomenology of the little Higgs model", *Phys. Rev. D* **67** (2003) 095004, doi:10.1103/PhysRevD.67.095004, arXiv:hep-ph/0301040.

[37] M. Schmaltz and D. Tucker-Smith, "Little Higgs theories", *Ann. Rev. Nucl. Part. Sci.* **55** (2005) 229, doi:10.1146/annurev.nucl.55.090704.151502, arXiv:hep-ph/0502182.

[38] M. Perelstein, "Little Higgs models and their phenomenology", *Prog. Part. Nucl. Phys.* **58** (2007) 247, doi:10.1016/j.ppnp.2006.04.001, arXiv:hep-ph/0512128.

[39] K. Agashe, H. Davoudiasl, G. Perez, and A. Soni, "Warped gravitons at the LHC and beyond", *Phys. Rev. D* **76** (2007) 036006, doi:10.1103/PhysRevD.76.036006, arXiv:hep-ph/0701186.

[40] L. Randall and R. Sundrum, "A large mass hierarchy from a small extra dimension", *Phys. Rev. Lett.* **83** (1999) 3370, doi:10.1103/PhysRevLett.83.3370, arXiv:hep-ph/9905221.

[41] L. Randall and R. Sundrum, "An alternative to compactification", *Phys. Rev. Lett.* **83** (1999) 4690, doi:10.1103/PhysRevLett.83.4690, arXiv:hep-th/9906064.

[42] ATLAS Collaboration, "Combination of searches for heavy resonances decaying into bosonic and leptonic final states using 36 fb$^{-1}$ of proton-proton collision data at $\sqrt{s} = 13$ TeV with the ATLAS detector", *Phys. Rev. D* **98** (2018) 052008, doi:10.1103/PhysRevD.98.052008, arXiv:1808.02380.

[43] CMS Collaboration, "The CMS experiment at the CERN LHC", *JINST* **3** (2008) S08004, doi:10.1088/1748-0221/3/08/S08004.

[44] CMS Collaboration, "Particle-flow reconstruction and global event description with the CMS detector", *JINST* **12** (2017) P10003, doi:10.1088/1748-0221/12/10/P10003, arXiv:1706.04965.

[45] CMS Collaboration, "Performance of electron reconstruction and selection with the CMS detector in proton-proton collisions at $\sqrt{s} = 8$ TeV", *JINST* **10** (2015) P06005, doi:10.1088/1748-0221/10/06/P06005, arXiv:1502.02701.

[46] CMS Collaboration, "Performance of CMS muon reconstruction in pp collision events at $\sqrt{s} = 7$ TeV", *JINST* **7** (2012) P10002, doi:10.1088/1748-0221/7/10/P10002, arXiv:1206.4071.

[47] CMS Collaboration, "Reconstruction and identification of $\tau$ lepton decays to hadrons and $\nu_\tau$ at CMS", *JINST* **11** (2016) P01019, doi:10.1088/1748-0221/11/01/P01019, arXiv:1510.07488.

[48] M. Cacciari, G. P. Salam, and G. Soyez, "The anti-$k_t$ jet clustering algorithm", *JHEP* **04** (2008) 063, doi:10.1088/1126-6708/2008/04/063, arXiv:0802.1189.

[49] M. Cacciari, G. P. Salam, and G. Soyez, "FastJet user manual", *Eur. Phys. J. C* **72** (2012) 1896, doi:10.1140/epjc/s10052-012-1896-2, arXiv:1111.6097.

[50] CMS Collaboration, "Pileup removal algorithms", CMS Physics Analysis Summary CMS-PAS-JME-14-001, CERN, 2014.

[51] M. Cacciari, G. P. Salam, and G. Soyez, "The catchment area of jets", *JHEP* **04** (2008) 005, doi:10.1088/1126-6708/2008/04/005, arXiv:0802.1188.

[52] CMS Collaboration, "Jet energy scale and resolution in the CMS experiment in pp collisions at 8 TeV", *JINST* **12** (2017) P02014, doi:10.1088/1748-0221/12/02/P02014, arXiv:1607.03663.

[53] D. Bertolini, P. Harris, M. Low, and N. Tran, "Pileup per particle identification", *JHEP* **10** (2014) 59, doi:10.1007/JHEP10(2014)059, arXiv:1407.6013.

[54] M. Dasgupta, A. Fregoso, S. Marzani, and G. P. Salam, "Towards an understanding of jet substructure", *JHEP* **09** (2013) 029, doi:10.1007/JHEP09(2013)029, arXiv:1307.0007.

[55] A. J. Larkoski, S. Marzani, G. Soyez, and J. Thaler, "Soft drop", *JHEP* **05** (2014) 146, doi:10.1007/JHEP05(2014)146, arXiv:1402.2657.

[56] CMS Collaboration, "Jet algorithms performance in 13 TeV data", CMS Physics Analysis Summary CMS-PAS-JME-16-003, CERN, 2017.

[57] J. Thaler and K. Van Tilburg, "Identifying boosted objects with N-subjettiness", *JHEP* **03** (2011) 015, doi:10.1007/JHEP03(2011)015, arXiv:1011.2268.

[58] CMS Collaboration, "Identification of double-b quark jets in boosted event topologies", CMS Physics Analysis Summary CMS-PAS-BTV-15-002, CERN, 2016.

[59] CMS Collaboration, "Identification of heavy-flavour jets with the CMS detector in pp collisions at 13 TeV", *JINST* **13** (2018) P05011, doi:10.1088/1748-0221/13/05/P05011, arXiv:1712.07158.

[60] J. Alwall et al., "The automated computation of tree-level and next-to-leading order differential cross sections, and their matching to parton shower simulations", *JHEP* **07** (2014) 079, doi:10.1007/JHEP07(2014)079, arXiv:1405.0301.

[61] D. Pappadopulo, A. Thamm, R. Torre, and A. Wulzer, "Heavy vector triplets: bridging theory and data", *JHEP* **09** (2014) 60, doi:10.1007/JHEP09(2014)060, arXiv:1402.4431.

[62] A. L. Fitzpatrick, J. Kaplan, L. Randall, and L.-T. Wang, "Searching for the Kaluza-Klein graviton in bulk RS models", *JHEP* **09** (2007) 013, doi:10.1088/1126-6708/2007/09/013, arXiv:hep-ph/0701150.

[63] W. D. Goldberger and M. B. Wise, "Modulus stabilization with bulk fields", *Phys. Rev. Lett.* **83** (1999) 4922, doi:10.1103/PhysRevLett.83.4922, arXiv:hep-ph/9907447.

[64] NNPDF Collaboration, "Parton distributions for the LHC Run II", *JHEP* **04** (2015) 040, doi:10.1007/JHEP04(2015)040, arXiv:1410.8849.

[65] T. Sjöstrand, S. Mrenna, and P. Skands, "A brief introduction to PYTHIA 8.1", *Comput. Phys. Commun.* **178** (2008) 852, doi:10.1016/j.cpc.2008.01.036, arXiv:0710.3820.

[66] T. Sjöstrand, S. Mrenna, and P. Skands, "PYTHIA 6.4 physics and manual", *JHEP* **05** (2006) 026, doi:10.1088/1126-6708/2006/05/026, arXiv:hep-ph/0603175.

[67] J. Alwall et al., "Comparative study of various algorithms for the merging of parton showers and matrix elements in hadronic collisions", *Eur. Phys. J. C* **53** (2008) 473, doi:10.1140/epjc/s10052-007-0490-5, arXiv:0706.2569.

[68] GEANT4 Collaboration, "GEANT4—a simulation toolkit", *Nucl. Instrum. Meth. A* **506** (2003) 250, doi:10.1016/S0168-9002(03)01368-8.

[69] J. Butterworth et al., "PDF4LHC recommendations for LHC Run II", *J. Phys. G* **43** (2016) 23001, doi:10.1088/0954-3899/43/2/023001, arXiv:1510.03865.

[70] T. Junk, "Confidence level computation for combining searches with small statistics", *Nucl. Instrum. Meth. A* **434** (1999) 435, doi:10.1016/S0168-9002(99)00498-2, arXiv:hep-ex/9902006.

[71] A. L. Read, "Presentation of search results: the $CL_s$ technique", *J. Phys. G* **28** (2002) 2693, doi:10.1088/0954-3899/28/10/313.

[72] CMS and ATLAS Collaborations, "Procedure for the LHC Higgs boson search combination in Summer 2011", CMS Note CMS-NOTE-2011-005, ATL-PHYS-PUB-2011-11, CERN, 2011.

[73] G. Cowan, K. Cranmer, E. Gross, and O. Vitells, "Asymptotic formulae for likelihood-based tests of new physics", *Eur. Phys. J. C* **71** (2011) 1554, doi:10.1140/epjc/s10052-011-1554-0, arXiv:1007.1727. [Erratum: doi:10.1140/epjc/s10052-013-2501-z].

[74] CMS Collaboration, "Combination of searches for heavy resonances decaying to WW, WZ, ZZ, WH, and ZH boson pairs in proton-proton collisions at $\sqrt{s} = 8$ and 13 TeV", *Phys. Lett. B* **774** (2017) 533–558, doi:10.1016/j.physletb.2017.09.083, arXiv:1705.09171.